

Dimensional optimization for the strength structure of a traveling crane

CAMELIA BRETOTEAN PINCA, GELU OVIDIU TIRIAN, ANA VIRGINIA SOCALICI,
ERIKA DIANA ARDELEAN

Department of Mechanical Engineering and Management
“Politehnica” University of Timișoara
Revoluției str., no. 5, Hunedoara
ROMANIA

camelia.bretotean@fih.upt.ro, ovidiu.tirian@fih.upt.ro, socalici.ana@fih.upt.ro,
ardelean.erika@fih.upt.ro

Abstract: - Most of the time, the strength structures who have not been statically determined, cut to the right sized, and checked out by the classic methods of the material strength cause the over sizing, because specialists use approximate measurements in order to decrease the number of mathematical calculation. This paper work describes the optimization of the main beam of a strength structure of a traveling crane used in metallurgy – by using the OPTSTAR mode that the COSMOS/M calculation software encloses which uses finite elements. In order to accomplish the best suited size, we have to perform both an analytic and experimental study about the performance of the traveling crane. In order to do that, we analyze the state of the tensions and deformation of the strength structure by using this calculation software based on COSMOS finite elements. In order to validate the analytic study, we have performed some industrial experiments by using specific devices for measuring the resistance of the electrical tension. Both the analytic and experimental studies have pointed out that we are able to come up with the best sizes in order to reduce the material consumption we used during the production process of the main beam within the strength structure of the traveling crane we have analyzed.

Key-Words: tension, traveling crane, optimization, deformation, over-sized, finite, elements.

1 Introduction

Most of the time, the strength structures who have not been statically determined, cut to the right sized, and checked out by the classic methods of the material strength cause the over sizing, because specialists use approximate measurements in order to decrease the number of mathematical calculation, [7], [8], [9],[14],[15], [16], [17].

Modern methods who use automatic data processing allow us to study the tension more accurately, especially due to the operative method of balance and continuity equation calculation, [1],[2],[7],[8],[19]. As far as the validity of the accuracy and operative method is concerned, they are real is the shaping up of the strength structure and the connection means are as good as possible [11], [12], [16]. This paper work describes the stages who make up the best dimensional optimization of the main beam who makes up the strength structure of the traveling crane. This device is installed in the hall of the Continuous casting Department of Hunedoara iron (and steel) works. In order to perform the best sizing for the product, we had to make both an analytical and an experimental study in order to see the way the traveling crane

works under tensions. The analytical study has been accomplished by the analysis of the tension and deformation stages of the strength structure of the traveling crane. We have used the calculation software based on COSMOS finite elements, [7], [8], [14], [15], [16], [19]. The analysis of the tension and deformation stages has been fulfilled by the authors in the paper works number [14] and [15]. This study has pointed out that we are able to perform the improvement of the product in order to reduce the material consumption.

In order to state the study is valid, we have to make an industrial experiment which should highlight the way the product works when used – it belongs to the strength structure of the traveling crane. The industrial experimental analysis has been performed by the resistance electrical tension measurement [16]. All experimental studies are important for:

- determining the tensions within the strength structure of the traveling crane under use, and of the distribution of the tensions within the area where the tension is concentrated. These areas are considered dangerous and they should be considered with the

most special attention when being designed and used.

- determining the highest values of the tensions for all situations.

The results of the experimental analysis are described in detail in the paper work [16].

The experimental study reveals that the way the strength structure works during the production stages is different from the calculation of the specialists, as far as the quantity is concerned; as far as the quality is concerned it is almost identical. The difference of quantity highlights the fact that the strength structure of the traveling crane has lower resistance features, so we must improve its features. The fact that they are equal in quality proves that the calculation method we have used for our theoretical study is valid [16]. After we have checked out the last limit state we have been able to consider the behavior of the strength structure of the traveling crane. We have performed this check up according to the results we have obtained due to the analytical and experimental analysis [1], [2], [7], [8], [16], [17]. Thus, the limit state of the working process of the strength structure of the traveling crane has been checked up in order to establish the best tensions and displacement by comparing the values we have determined by the experimental and analytical analysis, comprised in the above mentioned standards [1], [2], [7], [8], [14], [15], [16], [19]. The best aggregate feature of such a complex strength structure is important and difficult because there is a great number of equations we should solve, [2], [12]. Therefore, this paper work should refer to the method of finding the best features of the main beam within the strength structure [3], [10], [17]. Thus, we have come up with the most favorable size of the one longitudinal beam within the strength structure of the traveling crane- 100 KN –17,3 m. We have found the best size with the help of the OPTSTAR module belonging to the calculation COSMOS/M finite elements software, [18], [20].

2 Theoretical Concepts for the Most Favorable Method

As far as the design of the strength structures of metallurgic equipments is concerned, nowadays tendencies tend to find all the features that interfere with their use, in order to get the best solutions for complying with the resistance, the lastingness, and the most lucrative method [4],[16].

We find the best design of a strength structure if only we calculate the tensions and deformations caused by stresses. Due to such features, we would

be able to evaluate the whole structure, both statically and/or dynamically. We would also be able to design the size of all the elements, in order to provide the safety and the best working when stressed. Any of the calculation stages we use for determining the strength structures of such metallurgical equipments – comparing it to the conduct of the structure when stressed by specific values determined by the calculation method - has been influenced by the evolution and foundation substructures we needed to find the best method. From this point of view - [8], [16] - the calculation methods we have used for designing the strength structures of the metallurgical equipments could be classified into indirect and direct designing methods.

As far as the direct method is concerned, it is the method we use to find the size, the shape, and the raw material of the structure and the loads; and we should check out the behavior of the structure when stressed. Its behavior is influenced by tensions, deformations, mutations, cracks, and breaks. The structure is designed properly if all primary features of the estimated behavior are fulfilled; otherwise, we must change all the data – shape, size, and raw material – so that the features should be satisfying.

The direct method consists in determining the best size and type of material directly, so that they should not exceed the limit values that influence the working of the equipment.

The indirect designing method encloses the best method – we have described it in [16]. We consider it is the standard method. According to this method, the properties of the structure material, the geometrical features, the actions and stress are considered non-aleatory, since they have standard values, and the definition of the tolerable, σ_a , is possible if we measure it according to a unique security coefficient - c , who enables us to reduce the limit of material running. The only condition for the strength structure should not crack under stress and load, is that the highest tension - σ_{max} , - should not exceed a certain fraction of the running limit value. Choosing the security coefficient valid for any possible structure break is very important for the costs and the weight of the strength structure – they are often over-sized. Thus, choosing the determined design narrows the possibility of finding out the best method.

We had to use the statistic approach for any structure design, and in order to admit that the probability – we have used it in [4], is the most suitable method. The complete probability analysis of the resistance structure that all metallurgic equipments requires,[16] the statistic laws of load distribution and stress, of physical-mechanical

properties, geometrical sizes, and methods of the complete statistic calculation. The approach of the calculation procedure of the probability strength structures has some flaws which might be caused by a practical approach of the statistic theories we use for the current design of the complex resistance structures. It is difficult to use the practical method in order to find the most favorable probability method (we have described it according to the calculation methods of the strength structures [4],[5],[6],[16], and according to most of the cases of current design pattern), and it states the fact that the semi-probability concept is the second stage, meanwhile we find the calculation method – it is used to establish the bearing capacity - according to different security coefficients. We have called it the limit state method. The concepts and notions that the calculation method are defined by the norms [21], [22]. The method resides in providing the reasonable elements and the strength structures referring to the limit states who involve either loosing the feature of providing the use conditions or enabling some possible damage for people or goods [4].

According to [4], [16], the limit resistance states are divided into two categories:

- final limit states (they reach the highest values of the bearing capacity);
- normal use limit states (if the equipments reach these limits, they might damage the working of the equipment or of an element).

If we are able to define the two states, then we are able to calculate the strength structures during the designing and the working.

3 Improving Sub-structures

Nowadays, although there are several automatic calculus software based on finite elements, there may be certain high time values, if the structures are complex (of both data pre-processing and post-processing). Besides that, we should find the best method for those structures. In order to do that, we must use the calculus software several times - using a lot of entry data -, which might cause some major problems. In such cases, modern research use the sub-structure method. This method consists in dividing a complex structure into several segments, and considering they are independent items. The connection amongst the elements should be made according to the same pattern. Therefore, the sub-structure becomes an independent structure, and it has determined margin conditions which are required by the idea of a continuous initial structure. The problem of sub-structuring is described by the

specialized literature - [5], [6], [13] - and we should point out when we eliminate any stiff body movement of a unique structure. This structure is determined by the movement of the contour who represents the boundary amongst all substructures who have joint nodes. If we use the movement method, the structure is described by the stiffness matrix which is reduced to boundary nodes. In order to perform the study of the entire structure performance, we should connect the stiffness matrixes of all elements. There are two stages for such a performance. First of all, we connect the stiffness matrixes of the sub-structure elements, and then we reduce all joint nodes in order to perform the sub-structure connection within the stiffness structure matrix - [5], [6], [13].

We may face the same problem – sub-structures – in the case of big and complex structures, during the designing or the re-designing. For constructive and/or working purposes, we might not be able to change, re-design, improve, or turn it rigid, although the tension and deformation changes. Obviously, considering such conditions, the structure should be divided into sub-structures. In order to solve this problem, we use the condensation method. This method is common for all strength structures of a traveling crane who support the working systems, the order box, and all additional equipments who are made according to the best working conditions. The working should always improve in order to perform the highest stiffness while using the smallest quantity of raw material - [5], [6], [10], [13], [17]. Thus, we are able to solve the problem out faster, because if we divide it into several sub-structures, it allows us to reduce the breadth of the front, due to the fact that the analysis is not performed for the entire equipment, but for all sub domains. Except for the nodes, the separation line, the other nodes could be work offline, because they use conclusive balance equations. Thus, the nodes along the substructure line send the information to the rest of the structure; thus, all unknown elements are still working, [13]. The sub-structuring method described by specialized literature - [4], [5], [6], [8], [13] – follows the same arguments: blocking out the nodes, calculating the perfect fitting moments, unblocking the nodes, and following all the conditions required by the continuous spinning.

Dividing a complex structure into substructures consists in two stages:

- establishing the tension and deformation state for each substructure;
- coupling all substructures so that the connection areas should consider all balance features and movement.

Considering all above, this paper work is meant to provide the best sizing of the main beam of the strength structure of a traveling crane, based on the principle of substructures. Considering this study along with the previous studies – we have referred to them in the paperwork [14], [15], [16] – we are now able to perform the best sizing of a strength structure of a traveling crane, if we perform the best sizing of an end beam.

4 Numerical example of an oversized traveling crane

Metallurgical industry develops several technological processes whose features establish the type of equipment we should use to produce them – there are two categories: heavy and very heavyweight equipments. The technology we use for production determines the technological flow whose features call for using certain types of metallurgical equipments and transport and equipment jacking. The most usual equipments used in continuous cast plants are the rolling bridges. They differ according to their rigging-up from one industrial domain to another, and from a sector to another, within the same industrial domain, according to the characteristics of the technological process. Thus, we must choose the best pattern according to the requirements of the technological process. The main factors influence the way the equipment works, according to different loads that stress the strength structure of a traveling crane are: type of motion of the traveling crane structure, weight and type of the load, location of the traveling crane, geometric features and environmental conditions.

This current research has proven that the strength structure of a traveling crane we use in a casting line of a metallurgical plant.

The traveling crane we are analyzing is able to lift up to 100 KN, and the items are lift up to 17,3 m.

In the case of the particular travelling crane we are analyzing, the strength structure is made of locker-beams - both the two longitudinal beams and the two end beams. They made up a close-plan rectangular area, fig.1.

The longitudinal beams are very long and stressed, thus we make them according to a variable cross-section within the core of the beam, so that they could lift up the highest loads and work highly accurately. The height of the longitudinal beams is reduced at both ends, so they work like the „equal-resistance beams”, fig.2.

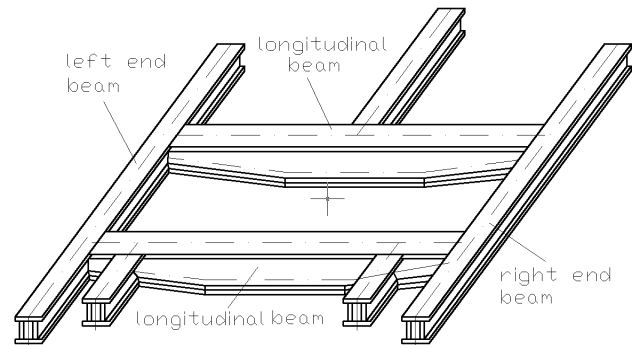


Fig.1 The strength structure of a travelling crane

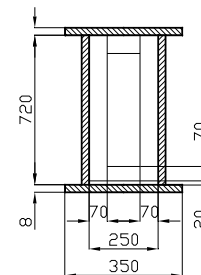


Fig.2 The cross section of the longitudinal beams

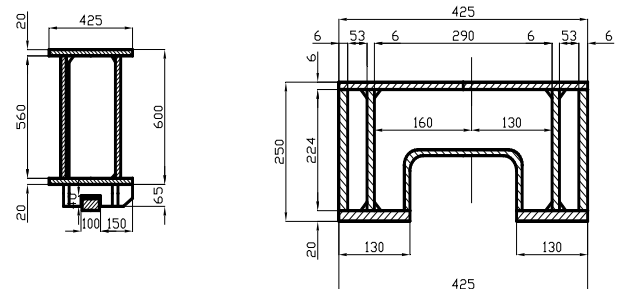


Fig. 3 The cross section along the end beams within the central and end area

The right and left end beams are concerned identical. This beams have a constant section along their lengths and they are made of some sheets welded to the locker, fig.3.

The design values used in the traveling crane analysis from the F.E.M and DIN standards are: lifting capacity: $G = 100$ KN; lifting height of 17,3 m; gauge of 11 m; distance between axes of 4,25 m; trolley velocity 10 m/min; traveling crane velocity 63 m/min; total duration of use U4; load spectrum class Q3; appliance group A5; loading type H (main load); dynamic coefficient $\psi = 1,15$; amplifying coefficient $\gamma_c = 1,11$. The cross section of the resistance elements is symmetrical and made of universal iron – they are weld together.

The strength structure of the traveling crane provides a certain static closed area. During the shaping up process, the presence of different

elements, the loads, and weight of the elements of the strength structure have been made up by concentrated weights; we have been able to change it with the help of some compressed forces, whose positions on the strength structure are described in fig.4.

The values of the forces are the following:

$F_1=4375\text{N}, F_2=9700\text{N}, F_3=9500\text{N}, F_4=5600\text{ N},$
 $F_5=2800\text{ N}, F_6=4215\text{ N}, F_7= 3375\text{ N}, F_8=31\ 489\text{ N},$
 $F_9=31\ 489\text{ N}, F_{10}=62\ 807\text{ N}.$

The position of the forces along the strength structure has been performed with the help of the following dimensions/sizes:

$a_1 = 1005\text{ mm}, a_2 = 3315\text{ mm},$
 $b_1 = 850\text{ mm}, b_2 = 400\text{ mm}, b_3 = 3970\text{ mm},$
 $l = b_1 + b_2 + b_3,$
 $c_2 = 850\text{ mm}, c_3 = 130\text{ mm}, c_4 = 825\text{ mm},$
 $c_5 = 180\text{mm}, c_6 = 2c_1 = 1120\text{mm}.$

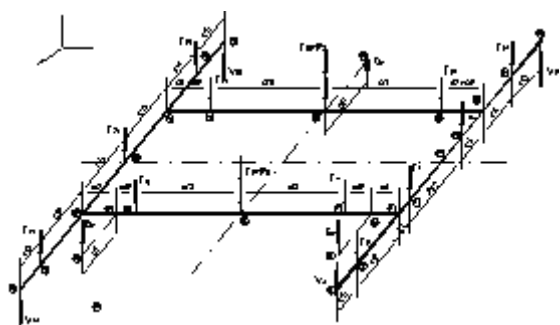


Fig.4 The pattern of the loading strength structure of a traveling crane

The loading static pattern is described in fig. 4 we need it to shape up the strength structure of the traveling crane in order to establish the type of tensions and deformations for finding the best sizing. This pattern has been performed according to the type and characteristics of all elements, as well as to the type of load taking over by each resistance element. In order to draw it out, we have considered the following elements:

- the space structure of the traveling crane is the result of the connection between two longitudinal and two end beams ; they are made of plane elements connected/situated orthogonally, on a vertical plan, and they make the side walls of the beams; meanwhile on a horizontal plane, they make the higher rack/plate, and the lower part of the beams;

- the phenomenon of space relationship is possible due to the fact that all the connections amongst the elements (which are situated on the vertical and orthogonal planes) are very accurate within the assembly of the strength structure of the traveling crane; that is possible because we need to

acknowledge the real tensions and deformations of the elements within a resistance structure whose space pattern requires us to consider the tridimensional co-operation amongst the elements.

The global analysis of the strength structure of any traveling crane has been completed for the less favorable positions of the loads. All the loads related to the elements, as well as those related to the entire strength structure of the traveling crane, have been considered basic elements for the physical shaping up of the strength structure, in order to establish the calculation pattern for the theoretical study of the tensions and deformations.

5 The solid model of traveling crane

Due to the complex structure of the resistance we have analyzed, it is difficult to choose the type of the finite element who we should use for producing a discrete item; and it is related to the way we are able to provide the continuous process amongst the elements. In this study finite element modeling is carried out by means of the Cosmos package,[18], [20] which has shell type elements with three or four nodes per element and six degrees per node in the finite elements library which secure a very good calculation accuracy, with deviations under 4 % related to the exact methods of calculation, [14], [15], [16]. The solid model of the traveling crane is presented in fig.5.

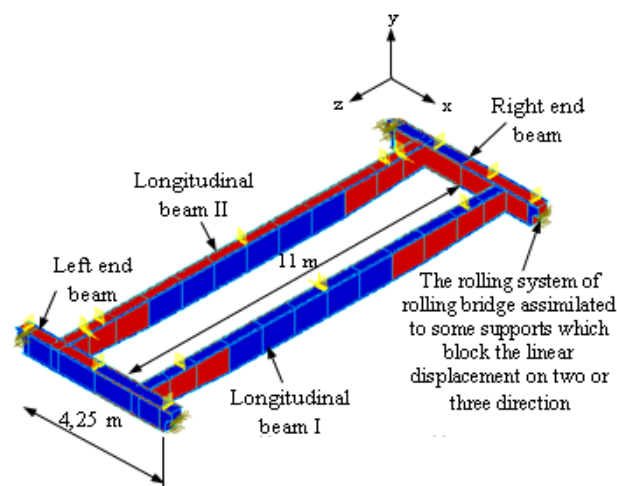


Fig.5 Solid model of the strength structure of the traveling crane

In the stage of the structure meshing here have been used a number of 42896 finite elements with a number of 20627 nodes and 12326 degrees of freedom. The big number of shell-type finite elements allowed us to come up with a calculation method which is almost similar to the real shape of

the strength structure we have analyzed. The geometrical model of the traveling crane has been elaborated in accordance with the workshop drawings, and the height number of elements of shell type used at meshing has allowed a calculation model very closed to the real geometry of the strength structure of the analyzed traveling crane.

The calculation method we have produced helped us make up a complete study about the tension and deformation state of the strength structure of the traveling crane and to highlight the detail of the focusing and the division of the tensions, as well as of their deformations caused by the working forces, [14], [15], [16].

4 Shaping-up the main beam

In order to find out the best method, we have shaped up the longitudinal beam I of the strength structure of that particular traveling crane we had been analyzing, based on the substructure principles.

In order to make the calculation, we have come up with the design of the longitudinal beam I – we have complied with the geometrical design and the operation process, [14], [15], [16]. The calculation pattern is described in fig.6.

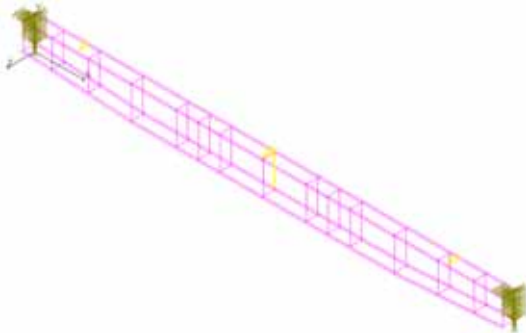


Fig. 6 The pattern of the calculation pattern used for the best sizing of the longitudinal beam I

In order to find the best method, the designing parameters are determined using the weight of the longitudinal beam – it should be very low –, if it complies with the designing restrictions we have described at *Sub point no. 5*. We have found the best sizing with the help of the OPTSTAR module, and it belongs to the finite-elements COSMOS calculation software.

5 Formulating the mathematical model/pattern/equation

The definite mathematical pattern for the problem of finding the best sizing for the longitudinal beam I we have considered the following elements:

- *designing variable features*: the width of the plate of the beams: $\delta_{min} < \delta < \delta_{max}$;

- *designing restrictions* – we consider the equivalent tension specific for the shaping up:

$$\sigma_{von\ Misses} < \sigma_{adm.};$$

- *the objective function* – the weight of the strength structure's of the beams: $G = G_{min.}$.

We have produced several different variants for the calculation software – the side cores. All the variants are the following:

- variant 2: $\delta_{t\ sup} = \delta_{t\ inf} = 7,5\ mm$ and $\delta_{i\ lat} = 6\ mm$;

- variant 3: $\delta_{t\ sup} = \delta_{t\ inf} = 7,5\ mm$ and $\delta_{i\ lat} = 5\ mm$;

- variant 4: $\delta_{t\ sup} = \delta_{t\ inf} = 6\ mm$ and $\delta_{i\ lat} = 6\ mm$;

- variant 5: $\delta_{t\ sup} = \delta_{t\ inf} = 6\ mm$ and $\delta_{i\ lat} = 5\ mm$;

- variant 6: $\delta_{t\ sup} = \delta_{t\ inf} = 5,5\ mm$ and $\delta_{i\ lat} = 6\ mm$;

- variant 7: $\delta_{t\ sup} = \delta_{t\ inf} = 5,5\ mm$ and $\delta_{i\ lat} = 5\ mm$.

The loadings have been considered in the elastic field, and therefore the elastic constants have been introduced, corresponding to the material OL 37.

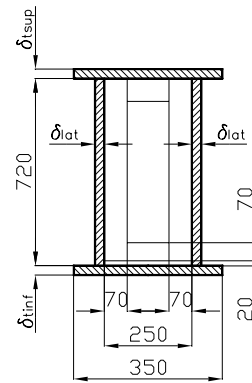


Fig.7 The cross section of the resistance elements

Variant 1 is considered the original variant, where: $\delta_{t\ sup} = \delta_{t\ inf} = 8\ mm$ and $\delta_{i\ lat} = 6\ mm$. Fig. 7 describes a cross section of the main beam, subject to our fitting. We have: $\delta_{t\ sup, inf}$ - the width of the upper bed plate, and the lower bed plate of the beam; $\delta_{i\ lat}$ – the width of the side cores of the beam.

6 Results

As a result of the calculation software based on finite elements for the variants we have already mentioned, we should enumerate the significant results of the fitting process. Table 1 contains the values of von Misses equivalent tensions valid for the four fitting variants for which we have maintained constant side cores and have changed the two bed plates of the longitudinal beam I (variants 1, 2, 4, 6).

Table 1. The highest values of the tensions within upper and lower bed plates of the longitudinal beam I for different „ δ ” widths

The analysis area	The resistance element	The width of the plate			
		8	7,5	6	5,5
		$\sigma_{\text{von Mises}} \text{ [N/mm}^2\text{]}$			
The middle of the longitudinal beam I opening	The upper bed plate	100,37	127,69	139,81	151,78
		78,36	95,78	107,61	120,11
	The lower bed plate	89,023	120,97	112,78	143,78
		91,31	117,65	121,96	123,25
The connection of the longitudinal beam I with the right end beam	The upper bed plate	87,73	138,12	147,12	159,74
		133,99	109,17	111,34	156,85
	The lower bed plate	108,94	134,72	139,9	153,71
		169,00	121,6	141,78	161,8

Table 2 contains the values of von Mises equivalent tensions for the longitudinal beam I, for those few nodes we have considered significant. They belong to the middle opening of the longitudinal beam I, more exactly to the connection area between this and the right end beam. The best variants we have analyzed and enclosed in this table are the original variant (variant. 1) and variant 7.

According to the analysis of the results enclosed into these tables, we are able to see that the values of the equivalent tensions which shape up the product increase as far as the width of the bed plates of the stringer decreases.

Table 2. The highest tension values for different nodes of the longitudinal beam I for different „ δ ” width

The analysis area	The width of the plate δ [mm]	
	6	5,5
$\sigma_{\text{von Mises}} \text{ [N/mm}^2\text{]}$		
The middle of the longitudinal beam I opening	50,34	60,87
	40,67	80,91
	31,003	47,6
	32,29	48,9
	30,9	80,54
The connection of the longitudinal beam I with the right end beam	168,90	161,08
	88,06	97,8
	128,56	134,57
	68,9	87,6

After we have studied and interpreted the results we had obtained, we have observed that the smallest size to reduce the width of the bed plates is 5.5 mm, and 5 mm (variant 7) for this fitting variant, the equivalent tensions which is specific to any reshaping for the longitudinal beam I goes between 20.135 N/mm² and 161.08 N/mm² fig. 8.

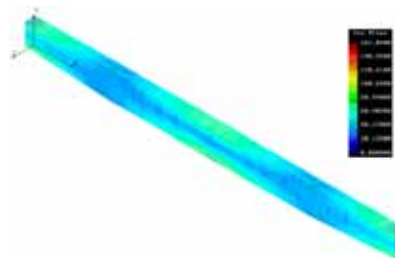


Fig.8 The distribution of the tension $\sigma_{\text{Von Mises}}$ for the fitted longitudinal beam I

As far as we see, von Mises equivalent tension reaches the highest values at the ends of the longitudinal beam, at the connection points with the end beams, at the upper bed plate and the lower bed plate – 161.08 N/mm². As far as the middle of their opening, we see that we have reached highest values at the level of the bin wings 143.78 N/mm² (sides of the lower bed plate), and at the connection point between the lower bed plate and the side core, we have 151.74 N/mm².

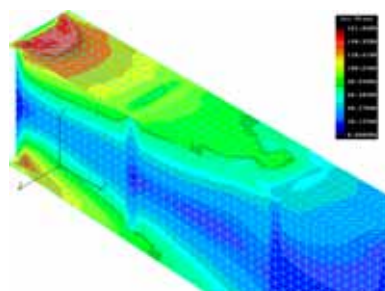


Fig.9 Details about the distribution of the $\sigma_{\text{Von Mises}}$ tension for the fitted longitudinal beam I at the connection area with the right end beam

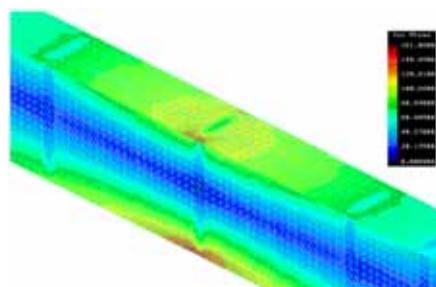


Fig. 10The distribution of the $\sigma_{\text{Von Mises}}$ tension for the fitted longitudinal beam I at the middle of the opening

When we analyze the values of this tension in detail, we that the fitted longitudinal beam I reaches extremely high tensions in the points where it is connected to the beams, fig. 9 – and at the middle of the opening, fig. 10.

As far as the resulting displacement, we see that the highest value after the fitting has been

performed reaches 10,20 mm, and it has been registered at the middle of the opening of the longitudinal beam I, fig. 11 and fig.12.

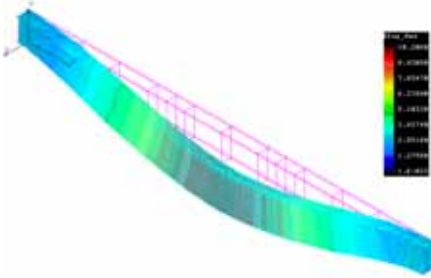


Fig. 11 The distribution of the resulting displacement on the fitted longitudinal beam I

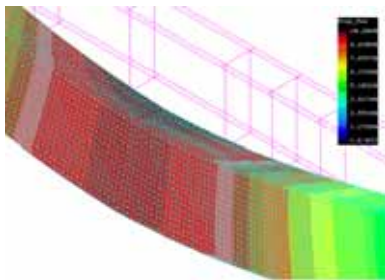


Fig. 12 Details about the resulting displacement on the fitting longitudinal beam I, at the middle of the opening

After we have analyzed the distribution of the results for the $\sigma_{\text{von Mises}}$ equivalent tension we have obtained after finding the best fitting with the results we have obtained by experimenting (we have described them in detail in [16]), we see that the difference amongst them reaches 10%. As far as the experiments are concerned, we have been able to perform them with the help of the resisting electrical tensiometry; for that reason the traveling crane has been loaded with steel lingots with specific precise weight. In the case of the strength structure we have analyzed, we knew the sizes of the cross-sections, and the fact that all the elements had been subject to static stress (their loads had been increased until they had exceeded the limit loads). The worst loading version was 120 KN - [16]. This confirms that the calculation pattern we have used is the best, [16].

For that version, we should calculate how much raw material we would use, and establish the percentage we are able to saved. We have to calculate the weight of the main beam according to the relation (1):

$$G = g \cdot \rho \cdot \sum_{i=1}^4 A \cdot l_i \quad (1)$$

This relation (1), contains the following

elements: G – total weight of the stringer, [kg]; g – gravitational speed, [m/s²]; A – cross-section area of an element of the stringer, [m²]; l – the length of the stringer, [m]; ρ - the density of the raw material, [kg/m³].

After we have calculated it, we have been able to reduce the weight of the I-type longitudinal beam with almost 8,46 % - for version no. 1 – and with 20,6 % - for version no. 7. In fig.13 we describe the highest equivalent tension variation of an element situated in the middle of the opening of the I-type longitudinal beam, which is situated on the lower plate, close to the connection point with the side core, and according to the weight „G” of the whole strength structure; we must also reduce the weight - ΔG .

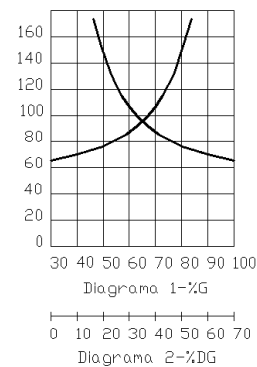


Fig.13 The variation diagram of the highest equivalent tension of an element situated in the middle of the opening of an longitudinal beam I

We have been able to perform some material reduction after performing this best fitting, and we have established the difference between the width of the stringer, before and after the optimization.

Comparing the tensions of the $\sigma_{\text{von Mises}}$ equivalent tension for the longitudinal beam I before and after optimization, we have come up with several results:

a) Before we have performed the fitting, we have had the highest values of the tension at the middle of the longitudinal beam I opening, for the upper bed plate, at the sides of the bin’s ends. But this area has the same high value – described in fig. 10, although we have performed the best fitting for von Mises equivalent tension;

b) We see that by reducing the width of the bed plates and of the cores, the equivalent tension increases;

c) Another area where we have high values of the equivalent tension is where the longitudinal beam I and the right end beam connect. The $\sigma_{\text{von Mises}}$ equivalent tension reaches the highest value of 182,89 N/mm². After we perform the best fitting, we reached some lower values than the first ones before performing the connection. This was possible due to the fact that the energies focused within the

connection point between the longitudinal beam I and the right end beam; the best fitting of the longitudinal beam I has been considered apart from the strength structure.

d) After we have performed the best fitting, as far as the resulting displacement is concerned, they reach lower values than those obtained by calculations. This was possible because they influence the difference of value. This could be caused by the fact that the longitudinal beam I is situated aside the rest of the structure of the traveling crane and the leaning conditions have not been yet well established. We are able to see that the right end beam we study is connected to the longitudinal beam II and the beams of the traveling crane and their nodes are rigid and depend on the stiffness of the concurrent beams. According to such conditions, the main beam due to investigations we can consider that they are fixed by some elastic beds; the displacement and the node turning are allowed by such a bed, we must determine that using additional calculations;

e) When comparing the values of von Misses tensions we have obtained after the fitting of the longitudinal beam I, and we have established the last limit values (already established according to the current norms), we see that the results do not exceed the valid values.

f) The way the pattern of the longitudinal beam I works is considered apart from the strength structure and its quantity differs from the real structure. As far the quality is concerned, the two are similar. The cause for the fact that the quantity is different is described by c and d. Thus, the pattern we have obtained allows us to produce some theoretical research we should then use for performing the best fitting of the strength structure.

g) As far as the theory is concerned, the variant number 7 is the best. From a technological point of view, it is not, because it does not adjust to the production possibilities of any iron plate we use for producing the strength structure's stringers for the traveling crane. Moreover, like the main beams of the strength structures, the width of the bed plates should reach more 2 mm than the core width, but not more than 2.5 times the width. Therefore, we consider the best variant of the longitudinal beam I of the traveling crane, the variant where the upper bed plates reach 7.5 mm, meanwhile the side cores have 5 mm – this is the best variant as far as the technology is concerned.

Considering any change of the width of the resistance walls of a cross-section – beam type – of the longitudinal beam I within a strength structure of the traveling crane, we should keep the same height

of the sections. Thus, we are able to perform the most favorable reduction of its weight, up to almost 20.6%. Practically speaking, if we consider the production technology of the plates we use for producing the bins, there's a reduction of 8.46 %, but without exceeding the resistance of the material.

In order to reduce the weight of the strength structure, we should find out other solutions for a better sizing, and they should refer to: the variation of beams' height or the variation of the bed plates' breadth. They are recommended to any other technological process.

7 Conclusions

In this paper work we have analyzed the best sizing of the main beam within the strength structure of a traveling crane that we use for the continuous casting in a metallurgy plant. The best method has been determined using the semi-probability concept; meanwhile the calculation method was the limit states-method. For this method, we had to reach the best bearing capacity of the strength structure. We were able to do that with the help of different security coefficients. Thus, we have considered that the walls of the cross-section (caisson-type) of the longitudinal beam I have changed their features, meanwhile the height of the sections remained the same; we have theoretically reduced its weight with almost 20,6% (considering the production technology of the plates that the caisson is made of), but practically we have reduced it to 8,46%, without exceeding the required resistance of the raw material.

References:

- [1] Alkin C., Imrak C.E., Kocabas H., Solid modelling and finite element analysis of an overhead crane bridge, *Acta Polytechnica*, Vol. 45 No. 3, 2005, pp. 61-67.
- [2] Alkin C., *Solid modelling of overhead crane bridges and analysis with finite element method*, M. Sc. Thesis, Istanbul Technical University, Istanbul, Turkey, 2004.
- [3] Al-Garni A.Z., Moustafa K.A.F., Javeed Nazami C.G. – Optimal control of overhead cranes, *Control Engineering Practice*, vol 3, Issu 9, pp. 1277 – 1284, Elsevier Science Ltd, 1995.
- [4] Ancău M., Nistor L. Numerical optimization techniques in computer-aided design, Technical Publishing House, Bucharest, 1996.
- [5] Bathe K.J – Finite elemente Methoden- Matrizen und linear Algebra, die Methode der finiten Elemente, Losung von Gleichgewichtsbediuenen und Bewegungsgleichungen, Springer Verlag, 1990.

- [6] Blumenfeld M – Introduction in the finite element methode, Technical Publishing House, Bucharest 1995.
- [7] Demirsoy M., Examination of the motion resistance of bridge cranes, PhD. Thesis, Dokuz Eylul University, Izmir, Turkey, 1994.
- [8] Gârbea D., Finite element analise, Technical Publishing House, Bucharest, 1990.
- [9] Ketill P., Willberger N.E, Application of 3D solid modelling and simulation programs to a bridge structure. PhD. Thesis, Chalmers University of Technology, Sweden.
- [10] Muhammad A., Muhammad H.A. Shahid P. – Optimization of Box Type Girder of Overhead Crane, „Global Design to Gain a Competitive Edge”, pp. 609 -618, Chapter 4, Publisher Springer London, ISBN 978-1-84800-238-8.
- [11] Moustafa K.A., Abou-El-yazid T.G., Load Sway Control of overhed cranes with load hoisting via stability analysis, *JSME Int. Journal*, Vol.39, Nr.1, 1996, pp.34-40.
- [12] Mladenova C.D., Mladenov I.M. An experiment in increasing the lifting capacity of the pouring side crane, *Journal of theoretical and applied mechanics*, Vol.38, No.3, 2008, pp. 201-2002.
- [13] Motica A.M., Numerical investigations of resistance, stiffness and vibration to batmant, *Mirton Publishing House Timișoara*, 1998.
- [14] Pinca B. C., Tirian G.O - *The analysis of the stresses and strains state of the strength structure of a rolling bridge for increasing its solidity*, 2nd International Conference on Engineering Mechanics, Structures, Engineering Geology, 22- 24 July, Rodos Island, Greece, 2009, pp.86-94.
- [15] Pinca B. C., Tirian G.O - *Finite element analysis of an overhead crane bridge*-2nd International Conference on Finite Defferences - Finite Elements- Finite Volumes- Boundary Elements, Tbilisi, Georgia, June 26-28, 2009, pp.51-56.
- [16] Pinca B. C., Optimization of a strength structure of a metallurgical aggregate, *PhD. Thesis, Politehnica University, Timișoara*, Romania, 2002.
- [17] Venetsamos D.T., Magoula E.A.T, Provatidis C.G.- Performance- based optimization of the welded box of a single girder overhead traveling crane according to EC3 and EC1, 5th World Congress on Computational Mechanics, 5th European Congress on Computational Methods in Applied Science and Engineering, Venice, Italy, 2008.
- [18] Zienkiewicz O.C, Taylor R. L., - *La method des elements finis*, AFNOR, Paris, 1991.
- [19] Yang Zun-hua, Jin Guang-zhen, 3DEFA analysis of metallurgy crane, *Journal of Hubei Politechnic University*, Vol.18, No.2, China, 2003.
- [20] COSMOS User's guide, Structural research analysis corporation, Santa Monica, 1999.
- [21] CTICM – EUROCODE NO.3 – Calcul des structures en acier. Regles generales et regles pour les batiments, V.2-1991.
- [22] DIN 1800 (Teil 1) - Allgemeine Entwurfsggrundlagen.